

Complexes of Lanthanide Nitrates with Bis(diphenylphosphino)methane Dioxide

Anthony M. J. Lees and Andrew W. G. Platt*

School of Sciences, Staffordshire University, College Road, Stoke-on-Trent, ST4 2DE, U.K.

Received March 18, 2003

The reactions of lanthanide nitrates, $\text{Ln}(\text{NO}_3)_3$, with bis(diphenylphosphino)methane dioxide, $\text{Ph}_2\text{P}(\text{O})\text{CH}_2\text{P}(\text{O})\text{Ph}_2$ (L), lead to complexes with three distinct classes of structure. At low ratios of Ln:L (<1:1.5) in acetonitrile the ionic complexes $[\text{Ln}(\text{NO}_3)_2\text{L}_2]^+[\text{Ln}(\text{NO}_3)_4\text{L}]^-$ (Ln = Pr, Eu) have been isolated. When carried out with a 1:2 or higher ratio in ethanol the reaction yields $\text{Ln}(\text{NO}_3)_3\text{L}_2$ (Ln = La, Ce) and $[\text{Ln}(\text{NO}_3)_2\text{L}_2\text{H}_2\text{O}]^+[\text{NO}_3]^-$ (Ln = Nd, Gd, Ho). Geometrical isomerism is found for the cations $[\text{Ln}(\text{NO}_3)_2\text{L}_2\text{H}_2\text{O}]^+$ and is attributed to the extent of hydrogen bonding to the coordinated water. Ligand redistribution occurs on heating in the solid state giving yellow solids in all cases. Crystallization of these materials from ethanol or acetonitrile gives $[\text{Ln}(\text{NO}_3)_3\text{L}_3]^{2+} \cdot 2[\text{NO}_3]^-$, which have been structurally characterized for Ln = Gd and Yb. Electrospray mass spectra indicate that extensive ligand exchange reactions occur in solution.

Introduction

Complexes of lanthanide nitrates continue to attract attention for their inherent interest in exploring the realm of structural variation among the 4f metals and as mimics for less accessible actinide complexes¹ of potential interest in nuclear waste treatment. Many multifunctional PO-based ligands have been examined and the structures of their lanthanide^{2–4} and actinide^{5,6} complexes reported. Solvent extraction properties of a variety of organophosphorus compounds with f-block metals have also been examined.^{7–13} Solvent extraction studies of lanthanides with tetra(*p*-tolyl)-

methylene diphosphine dioxide,¹⁰ where no complexes were isolated, indicate that compounds with 4:1 ligand-to-metal ratios for lighter lanthanides and 3:1 ratios for heavier lanthanides are formed. In further studies diphosphine dioxides, $\text{R}_2\text{P}(\text{O})\text{CH}_2\text{P}(\text{O})\text{R}_2$, and related ligands were examined in solution by EXAFS.¹⁴ With R = *p*-tolyl, holmium nitrate forms 2:1 complexes, while for R = octyl 1:1 complexes were formed.

In view of the lack of structural data we felt it important to study a relatively simple diphosphine dioxide, bis(diphenylphosphino)methane dioxide, $[\text{Ph}_2\text{PO}]_2\text{CH}_2 = \text{L}$, in order to establish fundamental structural properties. There are many examples of complexes in which monodentate phosphine and arsine oxides act as ligands to lanthanides, scandium and yttrium,^{15–19} and it is of interest to see how the constraining of the donor set into a relatively small bite angle ligand such as $[\text{Ph}_2\text{PO}]_2\text{CH}_2$ might change the resulting structures. The stability of the P–C bond makes this an attractive ligand to study from a structural point of view, in

* Author to whom correspondence should be addressed. E-mail: a.platt@staffs.ac.uk. Fax: +44 1782294986.

- (1) Bond, E. M.; Gan, X.; Fitzpatrick, J. R.; Paine, R. T. *J. Alloys Compd.* **1998**, 271–273, 172.
- (2) Gan, X.; Duesler, E. N.; Paine, R. T.; Smith, P. H. *Inorg. Chim. Acta* **1996**, 247, 29.
- (3) Paine, R. T.; Bond, E. M.; Parveen, S.; Donhart, N.; Duesler, E. N.; Smith, K. A.; Noth, H. *Inorg. Chem.* **2002**, 41, 444.
- (4) Gan, X. M.; Duesler, E. N.; Paine, R. T. *Inorg. Chem.* **2001**, 40, 4420.
- (5) Matonic, J. H.; Nue, M. P.; Enriquez, A. E.; Paine, R. T.; Scott, B. L. *J. Chem. Soc., Dalton Trans.* **2002**, 2328.
- (6) Bond, E. M.; Duesler, E. N.; Paine, R. T.; Neu, M. P.; Matonic, J. H.; Scott, B. L. *Inorg. Chem.* **2000**, 39, 4152.
- (7) Kulyako, Y. M.; Malikov, D. A.; Chmutova, M. K.; Litvina, M. N.; Myasoedov, B. F. *J. Alloys Compd.* **1998**, 271–273, 760.
- (8) Modolo, G.; Odoj, R. *J. Alloys Compd.* **1998**, 271–273, 248.
- (9) Hill, C.; Madic, C.; Baron, P.; Ozawa, M.; Tanaka, Y. *J. Alloys Compd.* **1998**, 271–273, 159.
- (10) Yaita, T.; Tachimori, S. *Radiochim. Acta* **1996**, 73, 27.
- (11) Bond, E. M.; Engelhardt, U.; Deere, T. P.; Paine, R. T.; Fitzpatrick, J. R. *Solvent Extr. Ion Exch.* **1997**, 15, 381.
- (12) Tan, Y. C.; Gan, X. M.; Stanchfield, J. L.; Duesler, E. N.; Paine, R. T. *Inorg. Chem.* **2001**, 40, 2910.

- (13) Arnaud-Neu, F.; Browne, J. K.; Byrne, D.; Mars, D. J.; McKervey, M. A.; O'Hagan, P.; Schwing-Weill, M. J.; Walker, A. *Chem. Eur. J.* **1999**, 5, 175.
- (14) Yaita, T.; Narita, H.; Suzuki, S.; Tachimori, S.; Shiwaku, H.; Motohashi, H. *J. Alloys Compd.* **1998**, 271–273, 184.
- (15) Deakin, L.; Levason, W.; Popham, M.; Reid, G.; Webster, M. *J. Chem. Soc., Dalton Trans.* **2000**, 2439.
- (16) Levason, W.; Patel, B.; Popham, M. C.; Reid, G.; Webster, M. *Polyhedron* **2001**, 20, 2711.
- (17) Hill, N. J.; Levason, W.; Popham, M. C.; Reid, G.; Webster, M. *Polyhedron* **2002**, 21, 1579.
- (18) Hill, N. J.; Levason, W.; Popham, M. C. *Polyhedron* **2002**, 21, 445.
- (19) Levason, W.; Newman, E. H.; Webster, M. *Polyhedron* **2000**, 19, 2697.

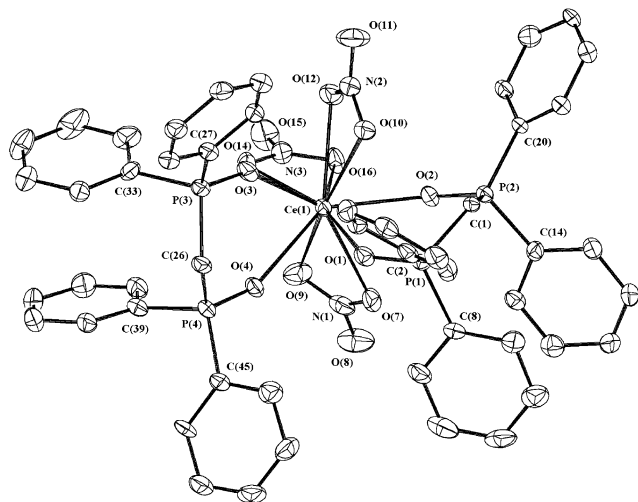


Figure 1. Structure of $[\text{Ce}(\text{CH}_2(\text{Ph}_2\text{PO})_2)_2(\text{NO}_3)_3]$ showing the atom-numbering scheme. Ellipsoids are drawn at the 50% probability level. Generated using SNOOPI.³²

that decompositions observed in bis-phosphonates $[(\text{RO})_2\text{PO}]_2\text{C}(\text{OH})\text{R}'^{20}$ cannot occur, while the presence of methylene protons between two electron-withdrawing phosphoryl groups holds potential for this ligand to behave as an acid on coordination to a metal, in a manner similar to acetylacetonone.

Results and Discussion

Synthesis and Solid State Structures. $\text{Ln}(\text{NO}_3)_3\text{L}_2$. For the reactions carried out with a 1:2 ratio of Ln:L the expected $\text{Ln}(\text{NO}_3)_3\text{L}_2$ resulted with structures which vary depending on the lanthanide metal. The complexes were all prepared by reactions of $\text{Ln}(\text{NO}_3)_3$ with L in ethanol or acetonitrile, although complexes suitable for X-ray crystallography were only formed from ethanol. The crystals of cerium complex used for structural analysis were formed by a different route, being isolated fortuitously from the reaction of ammonium cerium(IV) nitrate with L in acetone, the bulk material being a yellow amorphous powder which presumably contains Ce(IV).

Generally the structures show the effect of the lanthanide contraction in their overall constitution, with the lighter metals (La and Ce) giving neutral 10-coordinate molecular complexes, $\text{Ln}(\text{NO}_3)_3\text{L}_2$, while the smaller Nd and subsequent ions are 9-coordinate and ionic $[\text{Ln}(\text{NO}_3)_2\text{L}_2\text{H}_2\text{O}]^+[\text{NO}_3]^-$, an effect similar to that observed in the Ph_3PO complexes¹⁹ where the increased steric congestion results in the expulsion of a nitrate ion from the primary coordination sphere. The structures of the cerium and neodymium complexes are representative of the two classes and are shown in Figures 1 and 2, respectively. Details of the data collection and refinement for all the structurally characterized complexes and selected bond lengths and angles are given in the Supporting Information. The coordination mode of the complexes follows the same pattern as previously reported in the Ph_3PO complexes,¹⁹ with a donor set comprising 4

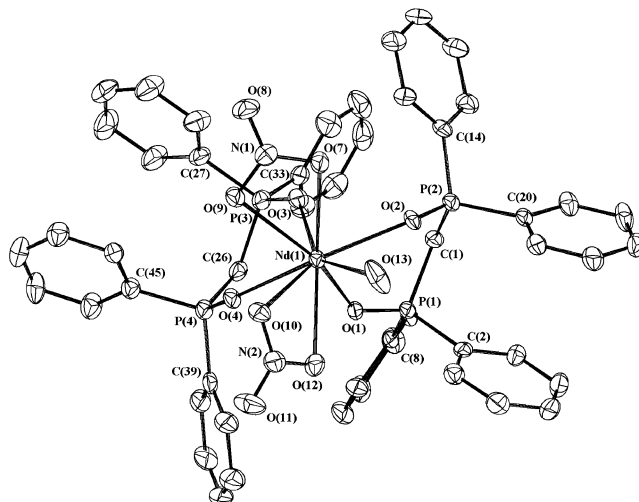


Figure 2. Structure of the cation $[\text{Nd}(\text{CH}_2(\text{Ph}_2\text{PO})_2)_2(\text{NO}_3)_2(\text{H}_2\text{O})]^+$ showing the atom-numbering scheme. Ellipsoids are drawn at the 50% probability level. Generated using SNOOPI.³²

$\text{P}=\text{O}$ and bidentate nitrate ligands. Not surprisingly the constraining of the donor set into the chelate ring forces a more acute $\text{P}-\text{O}-\text{M}$ angle from between 157° and 175° in yttrium nitrate complexes¹⁵ to between 138° and 146° here. The arrangement of the phosphine oxide donors is different from the pseudoplanar disposition observed in $\text{La}(\text{NO}_3)_3(\text{Ph}_3\text{PO})_4$. In our complexes the ligands adopt a pseudo cis configuration. This is indicated by the approximately 75° angle formed between the planes of the two PO bonds within each ligand (74.60° Nd, 75.20° Gd, and 75.65° Ho).

The lanthanide contraction is also apparent in the $\text{Ln}-\text{O}$ bond lengths, with linear decreases in $\text{Ln}-\text{OP}$ and $\text{Ln}-\text{ON}$ distances as a function of ionic radius of Ln^{3+} , with the distances to the nitrate ligand being consistently 0.06 \AA longer. These trends are shown in Figure 3.

Previously reported structures of $[\text{Ph}_2\text{PO}]_2\text{CH}_2$ complexed with NaBr^{21} and alkyltin halides²² contain chelating bidentate ligands as found here, with similar $\text{P}=\text{O}$ distances.

The geometry adopted by the chelate rings in the NaL_3^+ cation has the expected chair conformation of a cyclohexane ring. In our complexes the ring is flattened in the MO_2P_2 region with the Ln essentially in the $\text{P}_1-\text{O}_1-\text{P}_2-\text{O}_2$ plane. We attribute this change from idealized geometry to increased electrostatic repulsion between the metal ion and the positively charged phosphorus centers. Thus the $\text{Na}\cdots\text{P}$ distance of 3.69 \AA in the NaBr complex reflects a balance between the stability of the ring conformation and the electrostatic repulsion between Na^+ and the P atoms. Increasing the charge on the metal ion from +1 to +3 favors a structure in which the electrostatic $\text{M}\cdots\text{P}$ repulsion is reduced at the expense of the loss of the chair configuration. This conformation of the six-membered rings is quite constant throughout the range of structures determined, as discussed below, with only the gadolinium complexes showing slightly different ring conformations from the rest.

(20) Lees, A. M. J.; Charnock, J. M.; Kresinski, R. A.; Platt, A. W. G. *Inorg. Chim. Acta* **2001**, *312*, 170.

(21) Hewertson, W.; Kilbourn, B. T.; Mais, R. H. B. *J. Chem. Soc., Chem. Commun.* **1970**, 952.

(22) Pettinari, C.; Marchetti, F.; Cingolani, A.; Petinari, R.; Drozdov, A.; Troyanov, S. *Inorg. Chim. Acta* **2001**, *312*, 125.

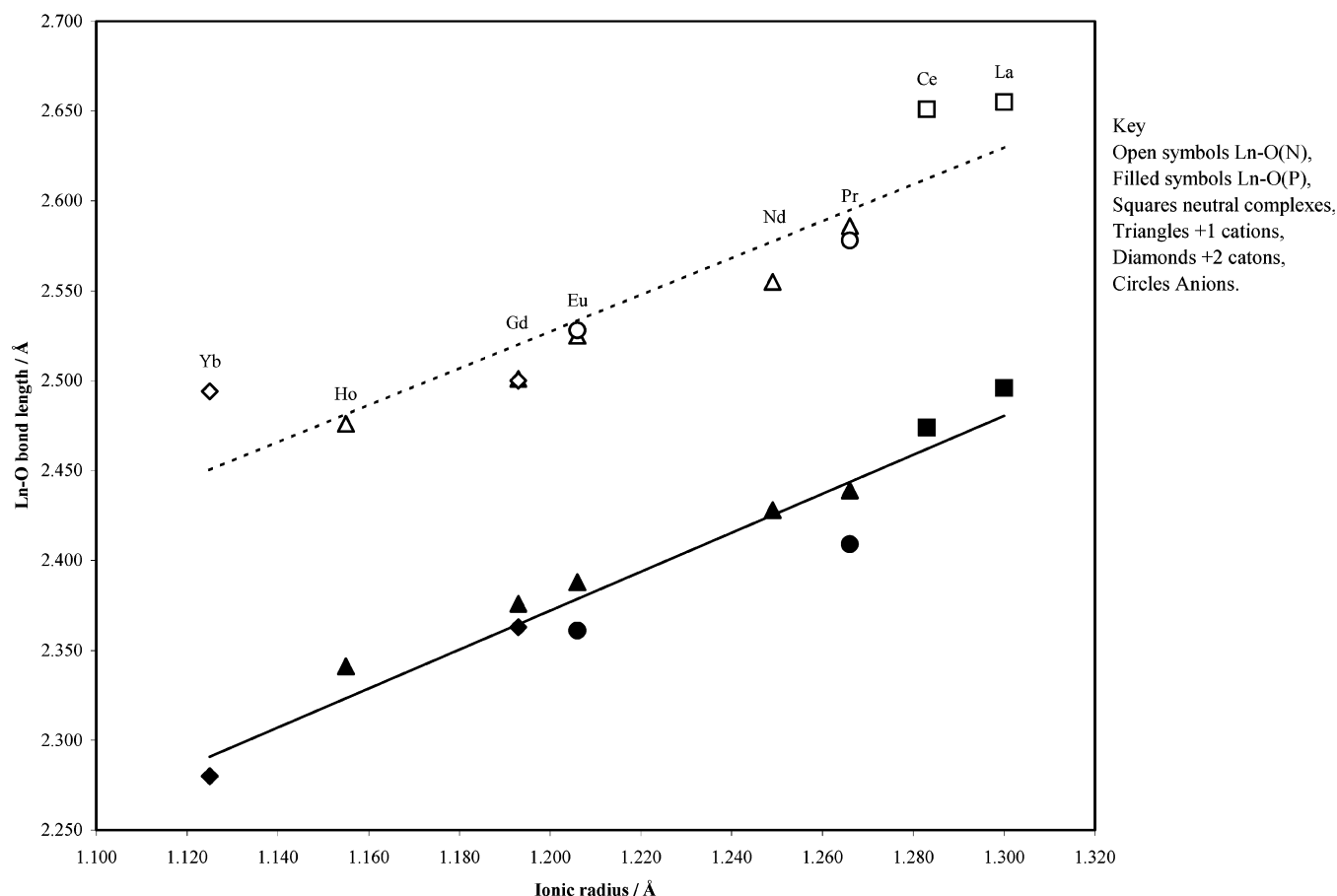


Figure 3. Correlation between mean Ln–O distances in DPPMO₂ complexes.

Hydrogen bonding is apparent in all of the structures. For the neutral complexes there is H-bonding between the EtOH and the terminal oxygen of one of the coordinated nitrates with an $\text{O}\cdots\text{O}$ distance of 2.788 Å for the La complex, which is well below the sum of van der Waals radii for oxygen. The cerium complex has a weak bonding interaction between the acetone oxygen and the methylene group of one of the chelate rings. Here the $\text{C}\cdots\text{O}$ distance of 3.255 Å is at the limit of the sum of van der Waals radii for carbon and oxygen and indicates a very weak interaction.

In the ionic complexes the H-bonding is more extensive, with the coordinated water in the cation bonded to nitrate ion and water (Nd, Gd) or nitrate and ethanol (Ho). The $\text{O}\cdots\text{O}$ distances all lie well below twice the van der Waals radius of oxygen. This network connects adjacent cations as indicated in Figure 4 and produces a hydrophilic side to the complex which includes the polar molecules and largely excludes the hydrophobic phenyl rings with only two of the eight in the vicinity of the hydrogen-bonding region. It is interesting to note that the methylene groups of the coordinated bis-phosphonate are directed away from the coordinated nitrate, in contrast to the structures of the cations in $[\text{Ln}(\text{NO}_3)_2\text{L}_2\text{H}_2\text{O}][\text{Ln}(\text{NO}_3)_4\text{L}]$ discussed below.

Finally for these complexes, the use of a Ce(IV) starting material in reaction leading to the isolation of the $\text{Ce}(\text{NO}_3)_3\text{L}_2\cdot\text{OCMe}_2$ gives rise to the possibility that this complex could, in principle, contain Ce(IV). Indeed it has

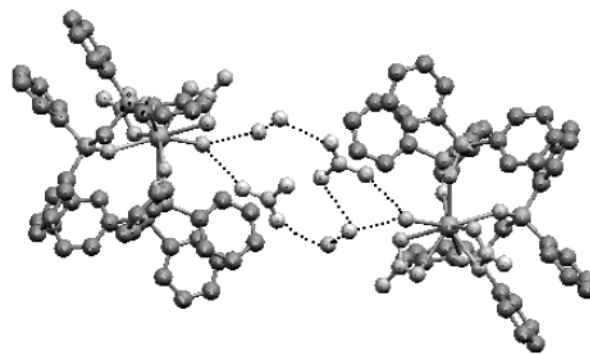


Figure 4. The hydrogen-bonding network connecting the cations in $[\text{Ln}(\text{NO}_3)_2\text{L}_2\text{H}_2\text{O}]^+[\text{NO}_3]^-$, Ln = Nd, Gd.

been recently pointed out that some oxidation state assignments have been incorrect, especially where loss of H^+ can lead to ambiguities, and that a more detailed analysis is required to assign the oxidation state of cerium with certainty.²³ The average Ce–O distance here is 2.580 Å, in good agreement with the average of 2.587 Å for 10-coordinate Ce(III). The bond valence sum²³ was also calculated, giving a value for the oxidation state of 3.24, further confirming that the complex is genuinely Ce(III).

$[\text{Ln}(\text{NO}_3)_2\text{L}_2\text{H}_2\text{O}][\text{Ln}(\text{NO}_3)_4\text{L}]$. With 1:1 and 1:1.5 ratios of Ln:L in acetonitrile, $[\text{Ln}(\text{NO}_3)_2\text{L}_2\text{H}_2\text{O}][\text{Ln}(\text{NO}_3)_4\text{L}]$ were isolated rather than 8-coordinate species such as $\text{Ln}(\text{NO}_3)_3\text{L}$.

(23) Roulhac, P. L.; Palenik, G. J. *Inorg. Chem.* **2003**, *42*, 118.

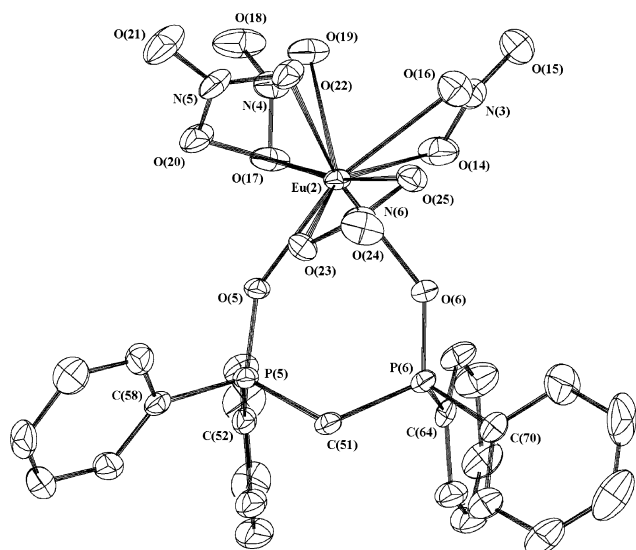


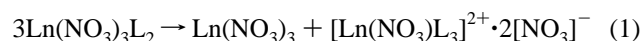
Figure 5. Structure of the anion $[\text{Eu}(\text{CH}_2(\text{Ph}_2\text{PO})_2(\text{NO}_3)_4)]^-$ showing the atom-numbering scheme. Ellipsoids are drawn at the 50% probability level. Generated using SNOOPI.³²

The structures of the praseodymium and europium complexes have been determined and are isostructural. The anion of the europium complex is shown in Figure 5. In these complexes the six-membered chelate rings adopt the same conformation in both cation and anion as observed for the $[\text{Ln}(\text{NO}_3)_2\text{L}_2]^+[\text{NO}_3]^-$ complexes. The Ln–O distances are consistent with the trends described above for the 1:2 complexes. In the $[\text{Ln}(\text{NO}_3)_4\text{L}]^-$ ions, the Ln–OP distances are 0.025 Å shorter than in their $[\text{Ln}(\text{NO}_3)_2\text{L}_2\text{H}_2\text{O}]^+$ -counterions; this is caused by the reduced steric repulsions due to the presence of only one L, permitting a closer approach to the metal.

Interestingly the relative positioning of the two chelate rings in the cations differs from that observed in $[\text{Ln}(\text{NO}_3)_2\text{L}_2\text{H}_2\text{O}]^+[\text{NO}_3]^-$, giving a rare example of geometrical isomers in lanthanide complexes. Thus the angle between the planes of the two PO bonds in each ligand, at about 153°, is roughly double that found in $[\text{Ln}(\text{NO}_3)_2\text{L}_2\text{H}_2\text{O}]^+[\text{NO}_3]^-$ (152.78° Pr and 152.96° Eu), indicating closer structural similarities with the triphenylphosphine oxide analogues with the O donors moving toward a planar arrangement. The structure of the cation in $[\text{Pr}(\text{NO}_3)_2\text{L}_2\text{H}_2\text{O}]^+[\text{Pr}(\text{NO}_3)_4\text{L}]^-$ is shown in comparison with that in $[\text{Nd}(\text{NO}_3)_2\text{L}_2\text{H}_2\text{O}]^+[\text{NO}_3]^-$ in Figure 6. For $[\text{Ln}(\text{NO}_3)_2\text{L}_2\text{H}_2\text{O}]^+[\text{Ln}(\text{NO}_3)_4\text{L}]^-$ the H-bonding of the coordinated water is limited to two of the acetonitriles, and thus any steric effects are limited to the second coordination sphere. In contrast to $[\text{Ln}(\text{NO}_3)_2\text{L}_2\text{H}_2\text{O}]^+[\text{NO}_3]^-$ there is no extensive hydrophilic region outside the primary coordination sphere, and as a result the phenyl groups are more uniformly distributed around the periphery of the ion and allow the P=O groups to move toward a relatively less congested pseudo-trans arrangement. Additionally, for the cations in $[\text{Ln}(\text{NO}_3)_2\text{L}_2\text{H}_2\text{O}]^+[\text{Ln}(\text{NO}_3)_4\text{L}]^-$ there is hydrogen bonding between the methylene protons of one of the ligands in the cation and nitrates, which with C···O(N) distances of 3.113 Å (Pr) and 3.106 Å (Eu) indicates only a weak hydrogen bonding (sum

of the van der Waals radii for C and O is 3.22 Å), but this could further lock the nitrate and phosphine oxide into the pseudo-cis geometry which is the principal difference in the structures of the cations. Further, the presence of $[\text{Ln}(\text{NO}_3)_4\text{L}]^-$ as a counterion compared to the “free” nitrate will also reduce the extent of H-bonding as the nitrate ions bound to Ln will be less basic.

$[\text{Ln}(\text{NO}_3)_3\text{L}_3]^{2+}\cdot 2[\text{NO}_3]^-$. On heating to 150 °C in the solid state the $\text{Ln}(\text{NO}_3)_3\text{L}_2$ complexes undergo reaction, changing color from that of the lanthanide ion to yield yellow solids in all cases. Washing the resulting solids with water gives compounds which analyze as $\text{Ln}(\text{NO}_3)_3\text{L}_3\cdot 2\text{H}_2\text{O}$. Crystals suitable for X-ray diffraction studies were grown from ethanol and acetonitrile for the gadolinium and ytterbium complex, respectively, and show that the complexes have the ionic composition $[\text{Ln}(\text{NO}_3)_3\text{L}_3]^{2+}\cdot 2[\text{NO}_3]^-$ and contain solvent molecules in the lattice. The structure of the gadolinium complex is shown in Figure 7. The thermal ligand redistribution reaction is interesting as we have been unable to form the same complexes by prolonged reaction of $\text{Ln}(\text{NO}_3)_3$ with excess L in solution. In some instances we have observed yellow solutions formed during crystallization attempts with a variety of lanthanide metals in a number of solvents. We have, however, so far been unable to isolate the tris complexes from these solutions, find any trend in their production associated with the metal, or reproduce the conditions for their formation. Our initial thoughts that the ligand had undergone a deprotonation reaction, possibly involving loss of HNO_3 , are not supported by the structures. The formation of tris complexes with scandium and lanthanide ions and even a tetrakis complex with lanthanum itself, all of which have the color of their respective lanthanide ion, is readily achieved using scandium and lanthanide triflates²⁴ where the lower coordinating ability of the anion allows the formation of LnL_3^{3+} and LaL_4^{3+} based cations even in low ligand-to-metal ratios. In the solid state the reaction appears to be as indicated in eq 1. The complex



$[\text{Eu}(\text{NO}_3)_2\text{L}_2\text{H}_2\text{O}][\text{Eu}(\text{NO}_3)_4\text{L}]\cdot 3\text{CH}_3\text{CN}$ also undergoes a similar ligand redistribution reaction on heating in the solid state. Thermal analysis of the process shows an endothermic loss of 6% mass at 140 °C corresponding to loss of the lattice CH_3CN and possibly H_2O .

The color of these complexes is unusual and was further investigated. The UV–visible spectra of the compounds in ethanol all show an absorption at $\lambda_{\text{max}} = 340 \text{ nm}$ that has a tail into the visible region which explains their yellow color. This absorption is much more intense than the f–f transitions from the metal ions, but less intense than the π – π^* from the aromatics and nitrate ions. This band is absent in solutions of the ligand itself, in ligand plus silver nitrate, and in $\text{Ph}_3\text{PO}\cdot\text{HNO}_3$, but is present in “L·HNO₃” (prepared as a yellow viscous oil by action of concentrated nitric acid on the bis-(diphenylphosphino)methane). Hydrogen bonding can be seen in the gadolinium complex between one of the “free”

(24) Fawcett, J.; Platt, A. W. G. *Polyhedron* **2003**, *22*, 967.

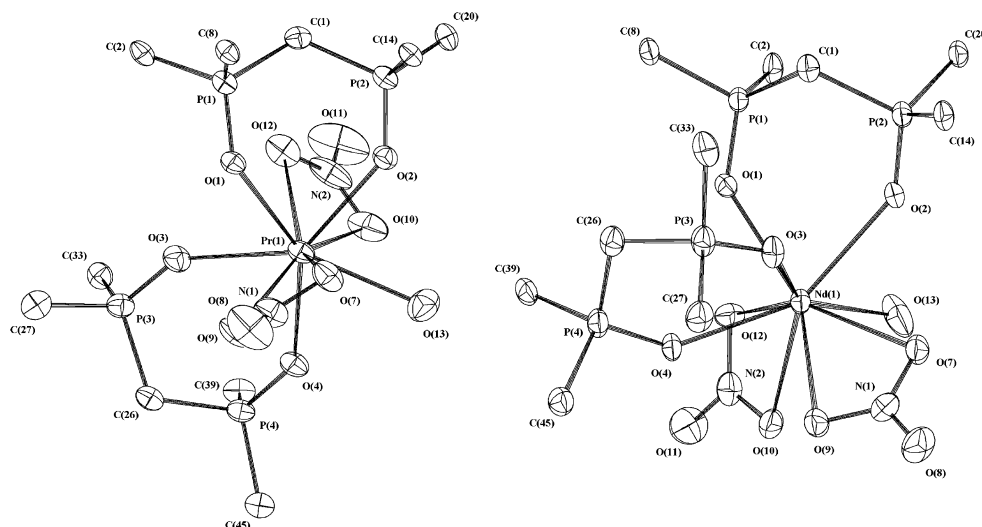


Figure 6. Structure of the cations $[\text{Ln}(\text{CH}_2(\text{Ph}_2\text{PO})_2)_2(\text{NO}_3)_2(\text{H}_2\text{O})]^+$ showing the atom-numbering scheme ($\text{Ln} = \text{Pr}, \text{Nd}$). Ellipsoids are drawn at the 50% probability level. Phenyl groups omitted for clarity. Generated using SNOOPI.³²

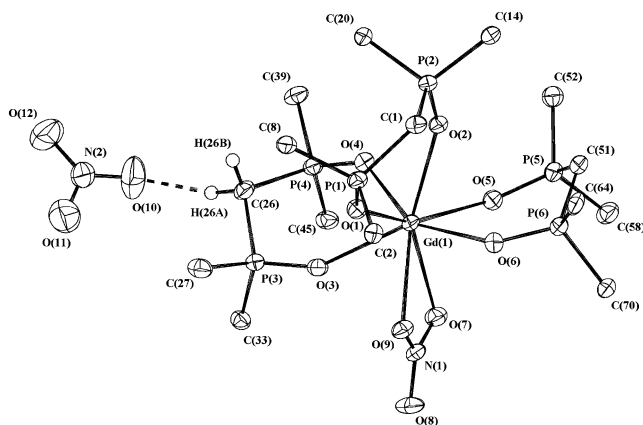


Figure 7. Structure of $[\text{Gd}(\text{CH}_2(\text{Ph}_2\text{PO})_2)_3(\text{NO}_3)_2]^{2+}$ showing the atom-numbering scheme and the hydrogen bonding between the methylene hydrogens and an ionic nitrate. Ellipsoids are drawn at the 50% probability level. Phenyl groups omitted for clarity. Generated using SNOOPI.³²

nitrate ions and the methylene hydrogens of one of the ligands (indicated by the dashed line in Figure 7); this nitrate is also hydrogen bonded to one of the ethanol molecules. The $\text{C}\cdots\text{O}$ distance in $\text{CH}_2\cdots\text{ONO}_2$ is 3.173 Å, which is slightly shorter than the sum of the van der Waals radii (3.22 Å). We have also observed similar hydrogen bonding between the triflate ion and methylene protons in the colorless $\text{ScL}_3(\text{OTf})_3$.²⁴ Hydrogen bonding between the phosphoryl oxygens and the $\alpha\text{-CH}_2$ groups in the solid state is well documented in the bis(phosphine) dioxides $\text{Ph}_2\text{P}(\text{O})\text{-}(\text{CH}_2)_n\text{P}(\text{O})\text{Ph}_2$ ($n = 2\text{--}8$).²⁵ There are no such interactions between CH_2 and PO in the $[\text{Ln}(\text{NO}_3)_2\text{L}_2]^+[\text{NO}_3]^-$ compounds, and we thus tentatively assign this band as arising from the interaction of the acidic ligand methylene protons with the “free” nitrate ion.

In these complexes the 8-coordinate cation can be considered to be a distorted octahedron formed by the oxygens of L capped by the nitrate ion. The $\text{Ln}\text{--}\text{O}(\text{P})$ distances are slightly shorter than in the other complexes while the $\text{Ln}\text{--}$

$\text{O}(\text{N})$ separations do not follow a consistent trend, being slightly shorter in the Gd complex but longer than expected in the Yb. However, the quality of the crystals of $[\text{Yb}(\text{NO}_3)_3\text{L}_3]^{2+}\cdot 2[\text{NO}_3]^-$ and the subsequent data mean that comparisons between the two structures can only be tentative.

Infrared Spectroscopy. The infrared spectra of the nitrate ion, in principle, provide a simple means of deducing information about its coordination to metals. While on local symmetry arguments alone it is not possible to distinguish between monodentate and bidentate nitrate, ionic nitrate should be readily identifiable. The spectra obtained for the complexes all show very similar nitrate absorption profiles which are more akin to those generally associated with coordinated nitrate. Thus the spectra show two well-separated series of bands for all the complexes, and there are no strong absorbances in the 1390 cm^{-1} region which could be assigned to ionic nitrate. This situation arises as a result of the hydrogen bonding, which lowers the local symmetry of all the “uncoordinated” nitrate ions. Thus in $[\text{Ln}(\text{NO}_3)_2\text{L}_2]^+[\text{NO}_3]^-$ and $[\text{Ln}(\text{NO}_3)_3\text{L}_3]^{2+}\cdot 2[\text{NO}_3]^-$ the $\text{N}\text{--}\text{O}$ bond lengths in the nitrates not directly bonded to the metals display considerable asymmetry. This is particularly evident when the nitrate is H-bonded to ethanol and thus the observed spectra are a superimposition of the spectra of H-bonded and bidentate coordinated nitrates. This illustrates the danger of assigning nitrate coordination modes by infrared spectroscopy alone when the potential for hydrogen bonding exists.

Electrospray Mass Spectra. The ESMS were recorded from solutions in methanol; assignments are based on the m/z ratio and the characteristic isotope patterns observed for many of the lanthanide ions. The data are summarized in the Supporting Information. The spectra show that extensive ligand redistribution reactions occur in solution despite the presence of chelating phosphine oxides. Ions representative of the solid state structures either are present in very low concentration for the cations in $[\text{Ln}(\text{NO}_3)_2\text{L}_2]^+[\text{NO}_3]^-$ or are entirely absent in the negative ion spectra of $[\text{Ln}(\text{NO}_3)_2\text{L}_2]^+[\text{Ln}(\text{NO}_3)_4\text{L}]^-$.

(25) Calcagno, P.; Kariuki, B. M.; Kichin, S. J.; Robinson, J. M. A.; Philip, D.; Harris, K. D. M. *Chem. Eur. J.* **2000**, *6*, 2338.

The base peak in most spectra is due to $[\text{Ln}(\text{NO}_3)_3]^{2+}$, an interesting observation as we have been unable to prepare complexes containing these cations from solutions of $\text{Ln}(\text{NO}_3)_3$ with excess L. It seems unlikely that the ML_3 and ML_4 based ions observed here are representative of the solution speciation, and it seems that the ionization conditions during the evaporation and droplet charging during the electrospray process favor the formation of the 3:1 dicationic complexes.

Within each ion type some simple trends relating to the ionic radius can be seen. The abundance of $[\text{ML}_4]^{3+}$ decreases from La to Yb, reflecting the increasing steric congestion such an ion would experience. A similar, though less pronounced, trend is seen in the relative intensities of signals due to $[\text{LnL}_4\text{NO}_3]^{2+}$. Loss of H^+ is apparent in the spectra of some of the complexes, appearing more pronounced for the lighter lanthanides. This is, perhaps, a little surprising since it might be anticipated that deprotonation would be more favored with the more polarizing heavier ions. Molecular modeling calculations were carried out on $[\text{ScL}]^{3+}$ and $[\text{YL}]^{3+}$ fragments to assess the gas-phase acidity of the methylene protons as a function of the size, and hence polarizing ability, of the metal ion. *Ab initio* calculations were carried out using an STO basis set. Both single-point and geometry optimization calculations were performed on mechanics-minimized structures with essentially identical results. The polarity of the C–H bond appears to be unaffected by the size of the metal ion, with charges of +0.11 and –0.38 on the hydrogen and carbon atoms, respectively.

Interestingly the geometry optimization calculation correctly predicts the observed conformation of the chelate rings with the methylene carbon lying above the mean MO_2P_2 plane.

The mass spectra from $[\text{Ln}(\text{NO}_3)_3]^{2+} \cdot 2[\text{NO}_3]^-$ ($\text{Ln} = \text{Gd}, \text{Er}, \text{and Yb}$) are slightly different from those obtained from $[\text{Ln}(\text{NO}_3)_2\text{L}_2]\text{NO}_3$, in that only lanthanide-containing ions with three or more ligands are observed. The tris chelate $[\text{Ln}(\text{NO}_3)_3]^{2+}$ gives the base peak in all spectra, indicating that the main solid state structural unit is retained in solution. Interestingly very low intensity signals (<1%) are also observed for $[\text{Ln}(\text{NO}_3)_2\text{L}_3]^+$ which possibly arise from a hydrogen-bonding interaction between $[\text{Ln}(\text{NO}_3)_3]^{2+}$ and nitrate ion of the type observed in the solid state. Signals are also observed from $[\text{Ln}(\text{NO}_3)_4]^{2+}$ (~20%) and weaker ones from $[\text{Ln}(\text{NO}_3)_5]^{2+}$ (~5%).

Conclusion

The structural studies show that, depending on the ratio of reactants, complexes $[\text{Ln}(\text{NO}_3)_2\text{L}_2]^+[\text{NO}_3]^-$ and $[\text{Ln}(\text{NO}_3)_2\text{L}_2]^+[\text{Ln}(\text{NO}_3)_4\text{L}]^-$ can be formed in which the cations have different geometries. This geometrical isomerization appears to be controlled by the hydrogen bonding between solvent molecules and the nitrate ions. Despite the formation of LnL_3 and LnL_4 complexes with counterions other than nitrate, no complexes with higher L:Ln ratios could be isolated from solution. Gentle heating in the solid state, however, led to the isolation of $[\text{Ln}(\text{NO}_3)_3]^{2+}$ complexes.

Experimental Section

X-ray Data Collection, Structure Determination, and Refinement. Data were collected by the EPSRC National Crystallography Service at the University of Southampton using previously described procedures.^{26–28}

For the La, Ce, Eu, Ho, and GdL_3 structures, the positions of the metal atoms were estimated using Patterson methods (SHELXS-97),²⁹ and all remaining non-H atom positions were obtained through subsequent Fourier syntheses (SHELXL-97).³⁰ Refinement was by full-matrix least-squares on F^2 data using SHELXL-97³⁰ from within the WinGX³¹ suite of software.

The GdL_2 and NdL_2 structures were refined by isomorphous replacement into the HoL_2 structure. In these two models the initial refinement of the ethanol molecule proved unstable, and following deletion of the EtOH atoms subsequent Fourier synthesis located peaks near to both the coordinated water molecule, O13, and the free nitrate group in each structure at distances consistent with the separation of hydrogen-bonded O atoms. Following assignment of these peaks as O, subsequent Fourier syntheses identified further peaks located roughly midway between O atoms, consistent with H-bonded water molecules. These were included as H atoms in subsequent cycles, restrained to give idealized H–O–H geometry.

In each of the structures, all non-H atoms were refined anisotropically with the exception of atoms C79 and N8 of one of the acetonitrile solvent molecules of the Pr structure and atoms O99, C98, and C99 of the ethanol molecule of the La structure.

All H atoms were refined at calculated idealized positions (phenyl C–H = 0.95 Å, methylene C–H = 0.98 Å, methyl C–H = 0.99 Å), and each functional group was assigned a single, refined isotropic displacement parameter. The H atoms of solvent molecules were assigned a common, refined H atom isotropic refinement parameter.

The non-centrosymmetric Ce structure refined to give a Flack absolute structure parameter of –0.019(8).

Data has been collected from further crystals obtained following the heating of Gd and Yb complexes to 150 °C overnight. The compounds appear to be isomorphous, and data suggests a monoclinic cell and space group $P2_1/n$. [Gd: $a = 22.4620$ Å, $b = 15.9106$ Å, $c = 45.3980$ Å, $\beta = 93.671^\circ$. Yb: $a = 22.4491$ Å, $b = 15.7437$ Å, $c = 45.2333$ Å, $\beta = 93.384^\circ$].

Models have been developed which show two similar $[\text{Ln}(\text{CH}_2(\text{Ph}_2\text{PO})_2)_3\text{NO}_3]^{2+}$ complexes in the unit cell of each compound. Two nitrate ions were readily located in each structure, but too many peaks remained in the difference Fourier maps to confidently assign further nitrate ions or solvent molecules.

Molecular Modeling Studies. The molecular modeling calculations were carried out using the SPARTAN V (version 4.1) package

- (26) Collect: Data collection software, R. Hoof, Nonius B.V., 1998.
 (27) Otwinowski, Z.; Minor, W. *Macromolecular Crystallography, Part A*; Carter, C. W., Jr., Sweet, R. M., Eds.; Methods in Enzymology; Academic Press: London, 1997; Vol. 276, p 307.
 (28) SORTAV absorption correction software package: (a) Blessing, R. H. *Acta Crystallogr.* **1995**, *A51*, 33. (b) Blessing, R. H. *J. Appl. Crystallogr.* **1997**, *30*, 421.
 (29) (a) Sheldrick, G. M. *SHELXS-97—A program for automatic solution of crystal structures*, release 97-2; University of Göttingen: Göttingen, Germany, 1997. (b) Sheldrick, G. M.; Dauter, Z.; Wilson, K. S.; Hope, H.; Sieker, L. C. *Acta Crystallogr.* **1993**, *D49*, 18.
 (30) Sheldrick, G. M. *SHELXL-97—A program for crystal structure refinement*, release 97-2; University of Göttingen: Göttingen, Germany, 1997.
 (31) (a) Farrugia, L. J. *WinGX—A Windows Program for Crystal Structure Analysis*; University of Glasgow: Glasgow, 1998. (b) Farrugia, L. J. *J. Appl. Crystallogr.* **1999**, *32*, 837.
 (32) Davies, K. *SNOOPI—Molecular plotting program*; Chemical Crystallography Laboratory, University of Oxford: Oxford, 1983.

on a dedicated Silicon Graphics work station. Geometry optimizations were carried out in two stages. Structures were first energy minimized using molecular mechanics force field and the structures thus produced further optimized by ab initio calculations using STO basis sets.

Electrospray mass spectra were obtained by the EPSRC National Mass Spectrometry Service Centre at University of Wales, Swansea, as described previously.³³

Infrared spectra were obtained on a Thermo Nicolet Avatar 370 FT IR. Crystals were removed and compressed onto a diamond window, and spectra were obtained without further sample treatment.

Synthetic Work. The ligand was prepared by oxidation of the phosphine with hydrogen peroxide in acetone solution. In a typical preparation hydrogen peroxide (10 mL 30% aqueous solution) was slowly added to an ice cold, stirred suspension of bis(diphenylphosphino)methane (15.20 g) in 150 mL of acetone. The mixture was allowed to warm to room temperature and stirred for a further 30 min. The mixture was boiled to reduce the volume to about 40 mL, cooled, and evaporated to dryness. The crude product was recrystallized from dichloromethane/diethyl ether to give a white crystalline solid (12.5 g, 77%).

Complexes were prepared by the same general methods. Some representative examples for each type of complex are given below. All complexes have the characteristic color of the lanthanide ion, except for $[\text{Ln}(\text{NO}_3)_3][\text{NO}_3]_2$, which are yellow.

Crystals suitable for single-crystal X-ray diffraction formed spontaneously ($\text{La}(\text{NO}_3)_3\text{L}_2$, $[\text{Ln}(\text{NO}_3)_2\text{L}_2]^+[\text{NO}_3]^-$, and $[\text{Ln}(\text{NO}_3)_2\text{L}_2]^+[\text{Ln}(\text{NO}_3)_4\text{L}]^-$) or by slow cooling of saturated ethanol or acetonitrile solutions for $[\text{Ln}(\text{NO}_3)_3]^{2+}\cdot 2[\text{NO}_3]^-$. The crystals of $\text{Ce}(\text{NO}_3)_3\text{L}_2$ were produced fortuitously in the reaction between $(\text{NH}_4)_2\text{Ce}(\text{NO}_3)_6$ and L in acetone where the colorless crystalline Ce(III) complex was formed amid an amorphous Ce(IV) bulk material and separated mechanically under the microscope.

Preparation of $\text{Ln}(\text{NO}_3)_3\text{L}_2$. **$\text{La}(\text{NO}_3)_3\text{L}_2\cdot\text{EtOH}$.** Lanthanum nitrate (0.51 g 1.23 mmol) in 8 mL of ethanol was mixed with the ligand (1.00 g, 2.04 mmol) in 10 mL of ethanol. The complex precipitated as a white powder 0.85 g (59%).

Anal. Required (found): C, 51.88 (52.46); H, 4.19 (4.16); N, 3.49 (3.48).

$\text{Pr}(\text{NO}_3)_3\text{L}_2\cdot\text{H}_2\text{O}\cdot\text{EtOH}$. Praseodymium nitrate (0.21 g 0.48 mmol) in 5 mL of ethanol was mixed with the ligand (0.42 g, 1.01 mmol) in 8 mL of ethanol. The precipitate was filtered off to give 0.46 g (83%) as a white powder.

Anal. Required (found): C, 51.03 (51.10); H, 4.28 (3.80); N, 3.43 (3.77).

From Acetonitrile. The same general procedure was followed for the preparation of all the complexes. Stoichiometric quantities of lanthanide nitrate in about 10 mL of CH_3CN and the ligand in 20 mL of CH_3CN were mixed. The resulting suspension was evaporated to dryness and the crude solid stirred with diethyl ether and filtered.

$\text{Ce}(\text{NO}_3)_3\text{L}_2$. Cerium nitrate (0.27 g, 0.62 mmol) in 10 mL of CH_3CN and the ligand (0.49 g, 1.18 mmol) in 20 mL of CH_3CN were mixed. Evaporation of the resulting suspension followed by stirring with diethyl ether and filtration gave the product as a cream solid (0.57 g, 83%).

Anal. Required (found): C, 51.82 (51.72); H, 3.83 (3.90); N, 3.63 (3.80).

$\text{Dy}(\text{NO}_3)_3\text{L}_2\cdot\text{CH}_3\text{CN}$. Dysprosium nitrate (0.22 g, 0.50 mmol) and the ligand (0.43 g, 1.03 mmol) treated in the same way as the cerium complex gave 0.50 g (82%) of the product as a white powder.

Anal. Required (found): C, 51.09 (51.30); H, 3.88 (3.92); N, 4.58 (3.75).

Thermal Ligand Redistribution. $[\text{Gd}(\text{NO}_3)_3]^{2+}\cdot 2[\text{NO}_3]^- \cdot 2\text{H}_2\text{O}$ and $[\text{Yb}(\text{NO}_3)_3]^{2+}\cdot 2[\text{NO}_3]^- \cdot 2\text{H}_2\text{O}$. A small sample of the $\text{Ln}(\text{NO}_3)_3\text{L}_2$ complex was heated to 150 °C overnight. The resulting yellow solid was washed with water and dried at the pump.

Anal. for the Gd complex: required (found) C, 55.32 (55.78); H, 4.33 (4.32); N, 2.58 (2.54).

Anal. for the Yb complex: required (found): C, 54.78 (54.86); H, 4.29 (4.21); N, 2.56 (2.54).

Acknowledgment. We are grateful to the Royal Society of Chemistry for support through the research fund, the EPSRC for use of the X-ray crystallography service at Southampton University, and the National Mass Spectrometry Service at Swansea University. We thank Mr. Steven Edwards for practical assistance with the cerium(IV) reaction.

Supporting Information Available: Tables giving details of the data collection and refinement, bond lengths and angles, and electrospray mass spectral data and assignments. This material is available free of charge via the Internet at <http://pubs.acs.org>. Crystallographic data for the structures reported in this paper have been deposited with the Cambridge Crystallographic Data Centre, CCDC numbers 205415 (La), 205416 (Ce), 205417 (Pr), 205418 (Nd), 205419 (Eu), 205420 (GdL_2), 205421 (GdL_3), and 205422 (Ho). Copies of this information may be obtained free of charge from The Director, CCDC, 12 Union Road, Cambridge, CB2 1EZ, U.K. (fax, +44-1223-336033; e-mail, deposit@ccdc.cam.ac.uk; <http://www.ccdc.cam.ac.uk>).

(33) Fawcett, J.; Platt, A. W. G.; Russell, D. R. *Polyhedron* **2001**, *21*, 287.